Kidney International, Vol. 15 (1979), pp. 640–650

Ultrastructural events in early calcium oxalate crystal formation in rats

MICHAEL J. DYKSTRA and RAYMOND L. HACKETT

Department of Pathology, School of Medicine, University of Florida, Gainesville, Florida

Ultrastructural events in early calcium oxalate crystal formation in rats. A model system is described for the induction of renal calcium oxalate crystals with intraperitoneal injections of sodium oxalate in rats. Early crystals are formed predominantly in cortical areas. Massive amounts of calcium are associated with this process, as demonstrated by potassium pyroantimonate staining. Actual crystal formation appears to be an involved process associated with calcium, oxalate, and cellular membranes. Although overt stone formation was not observed, we feel that the intimate involvement of membranes during crystal formation may be similar to that found in renal stones.

Aspects ultrastructuraux au stade précoce de la formation de cristaux d'oxalate de calcium chez le rat. Un modèle d'induction de cristaux d'oxalate de calcium au moyen d'injections intrapéritonéales d'oxalate de sodium est décrit chez le rat. Les premiers cristaux sont formés dans les régions corticales. Des quantités importantes de calcium sont impliquées dans ce processus comme le montre la coloration par le pyroantimonate de potassium. La formation de cristaux paraît un processus complexe impliquant le calcium, l'oxalate et les membranes cellulaires. Bien qu'il n'ait pas été observé de formation de calcul il paraît possible que l'implication des membranes au cours de la formation de cristaux existe aussi pour les calculs rénaux.

The formation of urinary tract calculi in man has been a noted health problem since the beginning of recorded history. The systematic collection of data during the last century suggests that less developed societies have a preponderance of uric acid, urate bladder stones, whereas the more industrialized areas of Western Europe and North America manifest stone disease in the form of renal stones that are primarily composed of calcium oxalate [1, 2]. Diet and water quality have been implicated as causative agents in stone disease by certain workers [3, 4], and others suggest that endogenous sources of oxalate are as important as exogenous [5, 6] sources, but as yet the basic mechanisms in calculogenesis have not been clarified.

Since calcium oxalate stone formation presumably is the result of a series of events beginning with the formation of calcium oxalate nuclei, numerous studies have dealt with the physicochemical parameters involved in the formation of calcium oxalate crystals [7–11]. In studies with synthetic urine, Doremus, Teich, and Silvis [12] suggested that the nucleation of slightly soluble salts dissolved in aqueous solutions takes place so rapidly that in less than 1 min almost all crystal nuclei are formed. Studies by Prien [13] with fresh urine revealed that calcium oxalate precipitated in the form of small (5 μ) crystals in normal urine but was found also in large crystalline aggregates in the urine of stone-formers. Gardner and Doremus [14] concluded that inhibitors in normal urine reduce the growth rate of calcium oxalate dihydrate and also decrease the aggregation of the di- and mono-hydrates. They suggest that normal urine permits only the formation of smaller crystals and aggregates of crystals which are easily passed from the system. Finlayson and Reid [15] offer evidence that calcium oxalate crystals formed in kidneys are too small to remain trapped long enough in tubules to serve as a nidus for stone formation. They further suggest that stone formation can begin only on particles that are somehow attached in the renal system.

Early work in Boyce's laboratory [16] revealed higher levels of a mucoprotein substance in the urine of stone-formers than it did in normal urine, and histochemical analyses of calcium oxalate stones [17] demonstrated that PAS- and colloidal iron-positive material, presumed to be matrix material, formed 2 to 4% of renal calculi as described by Boyce [18] and is consistently associated with renal stones. Spherical calcium bodies measuring 5 to 15

Received for publication September 11, 1978
and in revised form November 29, 1978

0085-2538/79/0015-0640 $02.20

Table 1. Sodium oxalate injection schedule and fixation regimen[a]

	15 min before fixation	30 min before fixation	60 min before fixation	6 hr before fixation	12 hr before fixation	24 hr before fixation
	no. of rats					
Sodium oxalate treated[b]						
3 mg	3	5	6	4	4	2
4 mg	—	—	4	2	4	2
5 mg	4	3	7	4	4	2
7 mg	—	—	4	2	4	4
9 mg	4	5	12	4	4	2
Saline controls	—	1	4	—	—	—
Ischemic controls	—	—	6	—	—	—

[a] There were 116 rats in the study.
[b] The sodium oxalate dose was given per 100 g body wt.

μ in diameter, which are found in the urine of stone-formers, also have mucopolysaccharides associated with them [19]. Recent ultrastructural investigations have revealed membranous, fibrillar. and vesicular material associated with calculi [20, 21], and also with calcium oxalate crystals formed in renal tubules [22].

We have undertaken an ultrastructural examination of the early events leading to the formation of calcium oxalate crystals. The rat was chosen for our experimental model because of the ease with which sodium oxalate injections induce the formation of calcium oxalate renal crystals [23, 24], and the belief that an understanding of the process of crystal formation will help provide clues to the processes involved in the formation of kidney stones typical of calculous disease.

Cytochemical techniques for the identification of calcium [25] along with x-ray analysis of the stain product and crystals in the kidney tubules have allowed us to pinpoint more accurately the earlier stages of calcium oxalate crystal formation. PAS-positive membranes, vesicles, and fibrillar material which we have found associated with calcium oxalate crystals in our experimental model are similar to those thought to be a part of the matrix found in urinary calculi [17, 21, 26].

Methods

Male Sprague-Dawley rats (each weighing 150 to 300 g) were acclimatized in our animal quarters for at least 10 days prior to use. They were injected intraperitoneally with 3, 4, 5, 7, and 9 mg of sodium oxalate per 100 g body weight in a 0.22 M solution of sodium oxalate in 0.9% saline. Control animals were injected with similar quantities of saline solution without added sodium oxalate. At various times following the sodium oxalate injections, the animals were anesthetized with pentobarbital, 0.1 mg/100 g of body weight, i.p. (50 mg/ml solution). The details of the fixation schedule are given in Table 1. Kidneys from all animals were examined by light microscopy. Electron microscopic and cytochemical studies were done on saline controls and experimental animals 15, 30, and 60 min after sodium oxalate injections.

Light microscopy. The kidneys were removed and a transverse central section from each was placed in alcoholic formalin. Alternatively, a similar section was removed from kidneys perfused with fixative prior to preparation for electron microscopy as described below. Paraffin sections of the fixed kidneys were stained with hematoxylin and eosin. Sections were examined with bright field or polarizing optics on a Leitz Dialux-20 microscope.

Electron microscopy. Kidneys to be examined ultrastructurally were fixed by retrograde perfusion via the aorta [27] or immersion-fixed with the formaldehyde-glutaraldehyde fixative of McDowell and Trump [28]. For routine electron microscopy, the tissue was washed several times in a 0.1 M cacodylate buffer (pH, 7.2), postfixed in 2% (weight per volume) osmium tetroxide in the same buffer, dehydrated in a graded ethanol series, put through several changes of 100% acetone, and embedded in Spurr's plastic [29]. Thick sections (0.5 μ) were stained with toluidine blue for examination with the light microscope. Ultrathin sections of the embedded tissue were examined unstained in the electron microscope or poststained with 2% (weight per volume) methanolic uranyl acetate, followed by Reynolds' lead citrate [30].

Digestions of calcium oxalate crystals. Thick sections of plastic-embedded tissue were dried onto clean glass slides and observed with the polarized light microscope as either 0.1 N hydrochloric acid or 0.1 M EDTA (pH, 4.3) was added dropwise and left for 15 to 60 min under continuous examination. During this period, the majority of birefringent crystalline material disappeared. These sections were then reembedded in fresh plastic, sectioned, and the fields containing birefringent material which had disappeared under the light microscope were examined with the electron microscope. Tissue samples also were taken from the primary fixative, rinsed several times in buffer, and treated with 0.1 N hydrochloric acid for 1 hour, postfixed, dehydrated, and embedded in the standard manner for electron microscopic examination.

Cytochemistry. Calcium was localized in the tissue at the ultrastructural level by adding 4% (weight per volume) potassium pyroantimonate (aqueous) to an equal volume of aqueous 4% (weight per volume) osmium tetroxide, adjusting the pH to 7.6 with 0.1 N potassium hydroxide and then adding the tissue. The tissue was rinsed three times (10 min each) in distilled water to remove the osmium contained in the primary fixative prior to immersion in the osmium and pyroantimonate mixture. As a control, selected samples of tissue were treated with 10 mM EGTA at pH 9.4 for 4 hours between the primary fixative and the osmium and pyroantimonate postfixation solution to remove calcium from the tissue. In a separate experiment, performed to eliminate nonspecific cellular necrosis as a possible factor in positive pyroantimonate staining, we subjected six animals to renal pedicle occlusion for 45 min followed by 15 min of reflow. Kidneys from these animals were prepared for electron microscopy and cytochemical studies as well.

X-ray analysis. Unstained ultrathin sections of tissue prepared as cited above were examined with an ORTEC 6230 x-ray analyzer attached to a Phillips 301 electron microscope. Sections (1000 Å) of human calcium oxalate calculi embedded in Spurr's plastic were examined by the same technique for comparison.

Results

Gross effects of sodium oxalate injections on rats. The visible effect of low doses (3 mg/100 g body weight) on the injected rats was minimal. As the quantity of injected sodium oxalate increased, the rats developed motor difficulties. At the highest level used (9 mg/100 g body weight), the rats exhibited partial dysfunction of hindquarter muscle groups and became lethargic for 5 or 6 hours in most cases. Their urinary output dropped, compared to that of controls, over 8 hours of observation. When surgery was performed, it was noted that small vessel breaks resulted in greater bleeding than was normal. The peritoneal cavity of experimental animals had considerable edema. The aorta appeared partially constricted, which made cannulation somewhat more difficult than it was in control animals.

Light microscopy. Examination of paraffin sections of perfused and immersion-fixed kidneys revealed that animals treated with the smallest amount of sodium oxalate (3 mg/100 g body weight) for the shortest period of time (15 min) had crystals in the three major areas of the kidney (cortex, medulla, papilla). The crystals were birefringent, and many were in the rosette or sheaf pattern characteristic of calcium oxalate. In perfused kidneys, the crystals were always within the tubular lumens (Fig. 1), appeared to be free in the intraluminal space, but occasionally were directly apposed to the brush border of proximal convoluted tubules. Frequently cellular debris was found associated with the crystals at all dosages. Higher concentrations of sodium oxalate resulted in progressively greater numbers of crystals in the kidneys, mainly cortical in distribution, larger crystals, and more cellular damage within the tubules. The maximum crystal distribution was reached at the 9 mg/100 g dose level to which the animal was exposed for 1 hour. In immersion-fixed kidneys, animals with 3 mg/100 g doses of sodium oxalate typically had collapsed tubules in the cortical and medullary regions at 12 hours after injection (Fig. 2), whereas those which received a 9 mg/100 g dose had tubules with more patent lumens containing amorphous cellular debris (Fig. 3). Animals examined at 1, 6, 12, and 24 hours showed a variable response. Those that received either 3 or 4 mg/100 g had crystals throughout the kidney after 1 hour (in low numbers) and after 6 hours had virtually cleared the kidneys of crystals. Animals receiving single injections of 5, 7, and 9 mg/100 had massive crystal deposition within the kidney at 1 hour, but chiefly cortical in distribution. As the dose increased, the number of crystals cleared from the tissue at 6, 12, and 24 hours after injection decreased. The cortex cleared first, followed by the medulla and papilla. At the highest dose, the kidneys still had extensive deposits of crystals in the cortex, medulla, and papilla after 24 hours.

Electron microscopy. Conventional fixation of

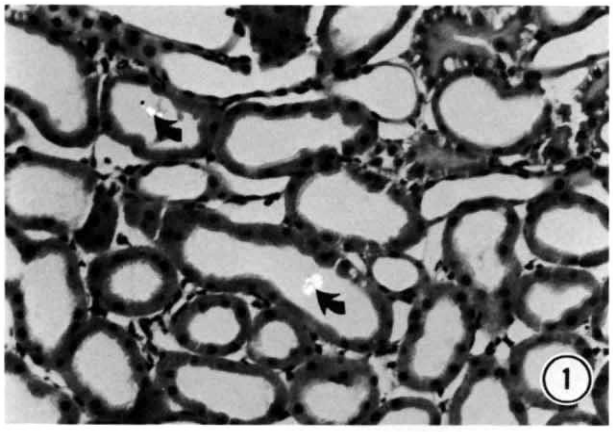

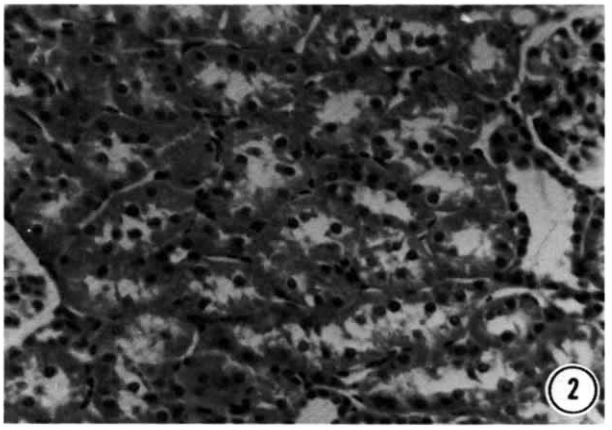

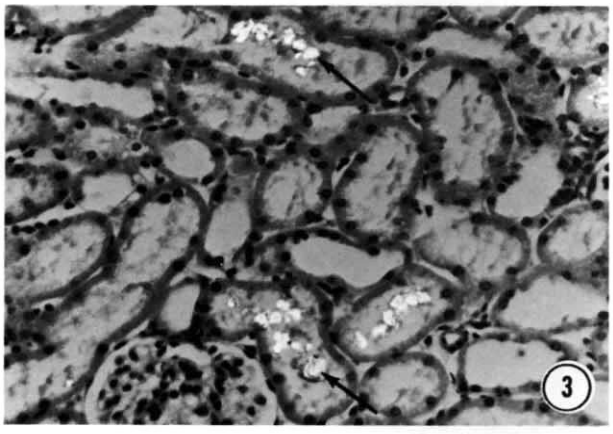

Fig. 1. *Light micrograph of cortical region of kidney from animal treated with sodium oxalate (NaOx) and then perfused with fixative, showing birefringent crystals* (arrows) *free in tubular lumens.* H & E section was viewed with partially polarized light (×225).

Fig. 2. *Light micrograph of cortical region of kidney from rat injected with 3 mg/100 g sodium oxalate, and immerse-fixed 12 hours later.* This H & E preparation was viewed with partially polarized light (×225).

Fig. 3. *Light micrograph of cortical region of kidney from rat injected with 9 mg/100 g sodium oxalate and immerse-fixed 12 hours later.* Note birefringent crystals within tubular lumens (*arrows*). This H & E preparation was viewed with partially polarized light (×225).

Fig. 4. *Electron micrograph of proximal tubule lumen from rat treated with 9 mg/100 g sodium oxalate.* Numerous holes (H) are left where crystals were pulled from the plastic and are surrounded by membranes (M) and pieces of microvillous-like (MVL) material (×13,500).

treated kidneys revealed two problems. The first was that the numbers of crystals in ultrathin sections of kidney tissue subjected to lesser levels of sodium oxalate were too few for systematic examination. Consequently, most observations are related to higher-dose animals, although crystal structure was identical at all doses used. The second problem concerned the difficulty of sectioning crystals of calcium oxalate, which were essentially uninfiltrated with plastic. The crystalline material was consistently pulled from the sections by the knife edge, resulting in distortion of the plastic and nearby tissue. It was still possible to see that membranes were associated with the crystals in luminal

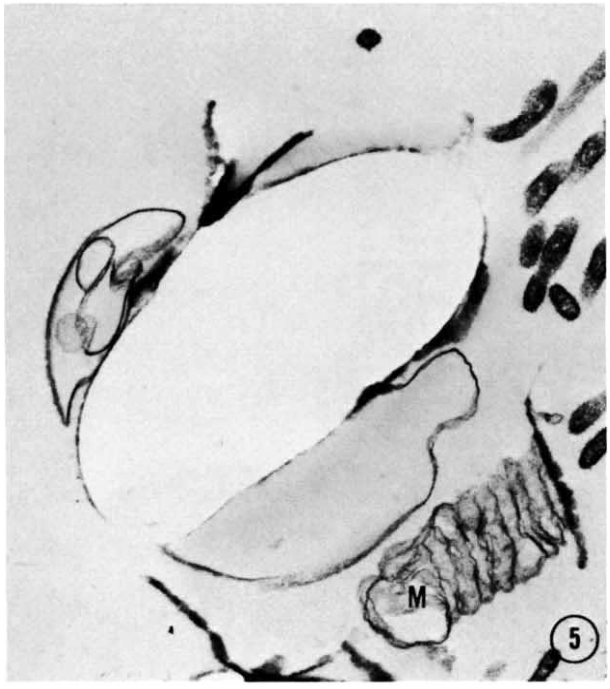

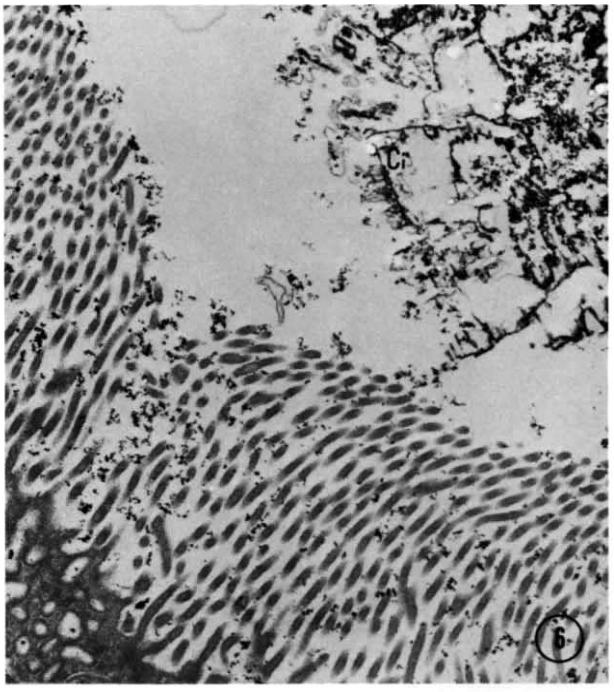

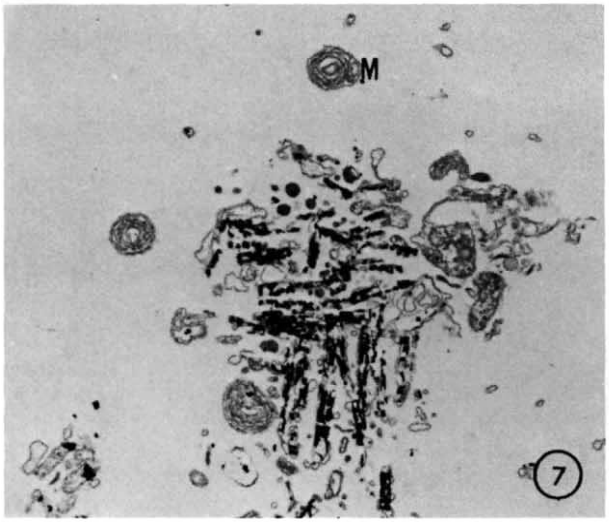

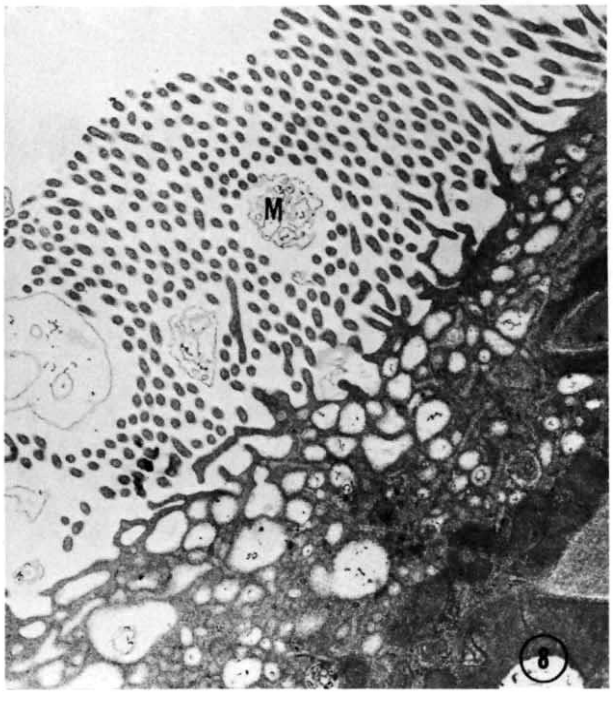

Fig. 5. *Electron micrograph of cortical tubule lumen with hole* (arrow) *left by crystal which was pulled from plastic during sectioning.* Note numerous membranes (M) associated with hole. Animals were treated with 9 mg/100 g sodium oxalate before fixation (×35,200).

Fig. 6. *Electron micrograph of proximal tubule with crystal in lumen (Cr) stained with pyroantimonate.* Stain product is also in between microvilli and in apical vesicles (×14,200).

Fig. 7. *Electron micrograph of crystal in tubule lumen stained with pyroantimonate.* Note whorls and pieces of membranes (M) associated with crystal (×10,950).

Fig. 8. *Electron micrograph of proximal tubule of rat perfused 1 hour after receiving 5 mg/100 g sodium oxalate.* Tissue was stained with pyroantimonate. Membranes (M) associated with microvilli and in apical vacuole are shown (×14,150).

spaces, but the actual physical relationship of the membranes to the crystals was partially obscured (Fig. 4 and 5). Similar difficulties have been illustrated by others [22].

For routine electron microscopy, digestion with hydrochloric acid or EDTA was done. This treatment eliminated the tearing problem associated with intact crystals and did not appear to affect the disposition of the membranous and fibrillar material associated with the crystals. An unexpected dividend of pyroantimonate staining, however, was that crystalline material that stained also sectioned easily, and the pulling and tearing artifacts associated with the untreated crystal was fortuitously eliminated (Fig. 6). Vesicular, membranous, and fibrillar material was always associated with crystals (Figs. 4 to 7). Membranes were frequently present within the tubular lumens prior to the actual appearance of crystals (Fig. 8).

Cytochemical localization of calcium in cortical tissue by the use of potassium pyroantimonate demonstrated the presence of presumed calcium at all sodium oxalate dose levels (Table 2). Increasing the amount of injected sodium oxalate and the length of exposure was associated with an increase in the quantity of stain product found. With high doses of sodium oxalate (9 mg/100 g), in animals perfused 60 min after injection, stain product appeared in the proximal tubular lumens (Figs. 9 and 10), apical vesicles, vacuole system of the proximal tubules, and among the microvilli of the brush border [6, 9, 10]. It was also heavily deposited on crystals (Figs. 6 and 7), associated with membranous sacs within the apical vesicle and vacuole system, and the tubular lumen (Fig. 8). Stain also was found sometimes in interstitial spaces near the peritubular capillary system, and occasionally in the urinary space of the glomerulus (Fig. 11). Flocculent material in some tubular lumens stained with pyroantimonate though the majority of such materials did not (Figs. 9, 10). Lower concentrations of sodium oxalate to which the animals were exposed for a shorter time resulted in sporadic staining with the pyroantimonate method. Some tubules showed no staining at all, whereas others had reduced amounts of stain product in all the same locations as in animals treated with heavier doses. After 60 min at all dose levels, stain product was associated with cell types and cellular components listed above.

Pyroantimonate treatment of kidneys from animals subjected to 9 mg/100 g for 60 min, perfused, and then soaked in EGTA for 4 hours revealed no staining in any part of the proximal tubules (Fig. 12) or other parts of the nephron. Occasional calcium oxalate crystals in tubular lumens that had not had all their calcium component removed by the EGTA still stained to some extent. Kidneys from normal animals, and saline and ischemic controls, which were perfused with fixative, showed no staining after pyroantimonate treatment (Fig. 13).

Energy dispersive (x-ray) analysis. Ultrathin sections of rat kidney cortex containing crystals were examined to determine if the crystals contained calcium. These studies demonstrated that the major component of the crystals was calcium, with no discernible magnesium. Readings taken of the particulate stain product in the apical vesicle and vacuole system of proximal tubules in crystal-bearing tissue were questionable due to the low counts per minute generated by the sparse stain product, but a slight shoulder was indicated in the region of calcium. Nuclei and cytoplasm of the proximal tubular cells well below the apical vesicle and vacuole system in animals subjected to 9 mg/100 g doses for 1 hour were scanned for the presence of calcium with the microprobe and revealed none.

Discussion

These experiments were done to investigate the early structural events occurring in the formation of calcium oxalate crystals in the kidney tubule. The advantage of the intraperitoneal method described

Table 2. Deposition of stain product in proximal tubules of perfused kidneys[a]

	Perfused 15 min after injection	Perfused 30 min after injection	Perfused 60 min after injection
Sodium oxalate treated[b]			
3 mg	+	++	++
5 mg	+	++	++
9 mg	+	+++	++++
Saline controls	(No staining product found anywhere in tissue)		
Ischemic controls	(No staining product found anywhere in tissue)		

[a] One plus (+) is the least amount of staining; four plus (++++) is the most amount of staining.
[b] The sodium oxalate dose was given per 100 g body wt.

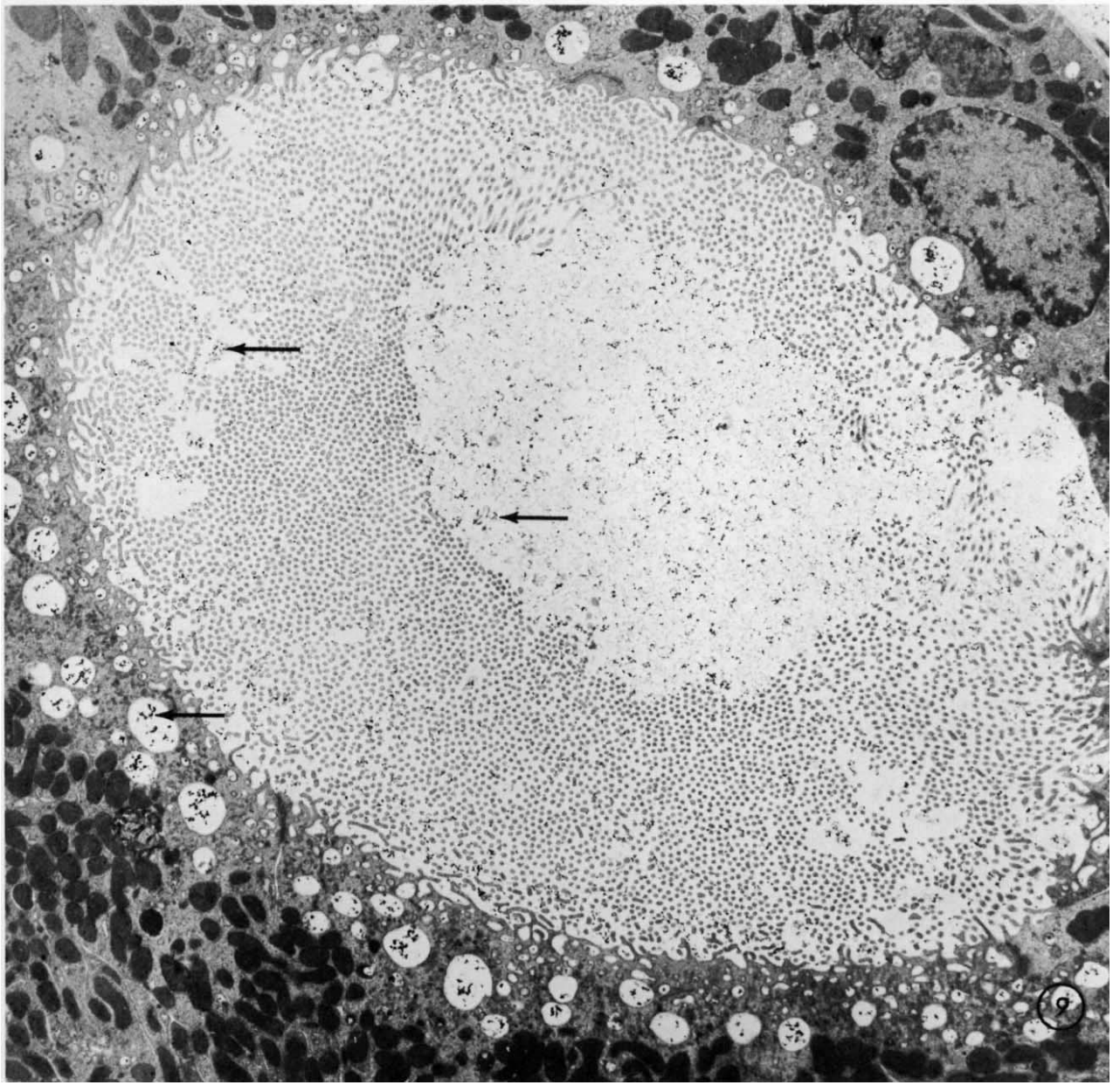

Fig. 9. *Electron micrograph of proximal tubule of rat fixed 1 hour after receiving 9 mg/100 g sodium oxalate.* The tissue is stained with pyroantimonate to reveal product in the apical vesicle and vacuole system, among microvilli, and in the tubular lumen (*arrows*) (×7920).

here, as compared to previous models, is the rapidity and constancy with which crystal formation can be induced. Although the quantities of sodium oxalate administered to the rats in our studies clearly provides an oxalate challenge greater than that encountered in human stone disease, we feel that the obtained results still provide us with important information about early formation of crystals that might be extrapolated to clinical conditions. The potassium pyroantimonate procedure provided an excellent ultrastructural detail of the crystals and did not affect ultrastructural analysis of cells. The method is for calcium ions, however, and we have no direct method for demonstrating the participation of oxalate ions in the formation of the crystals. Inferentially, the crystals are calcium oxalate, because they have the characteristic birefringent pattern associated with calcium oxalate.

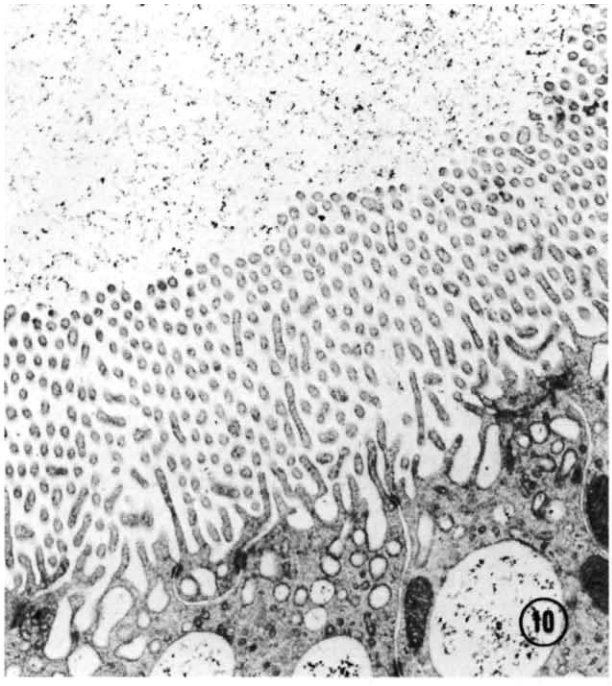

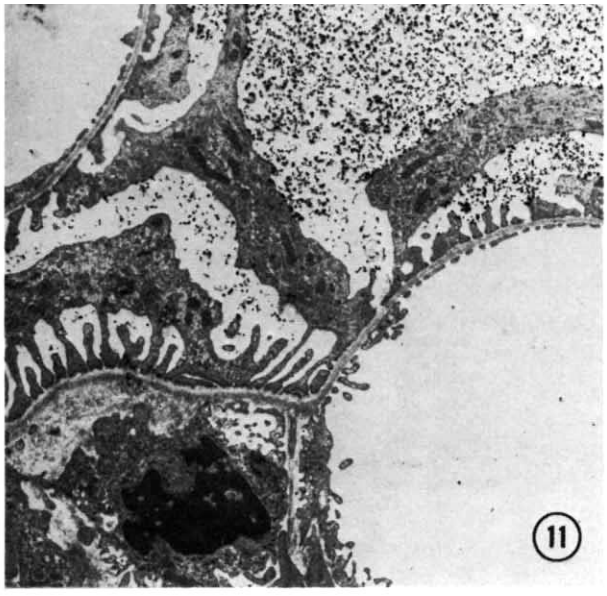

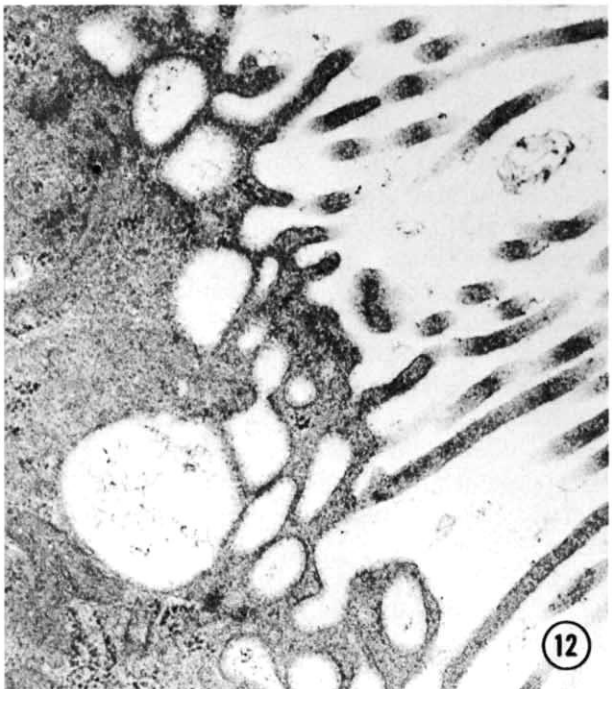

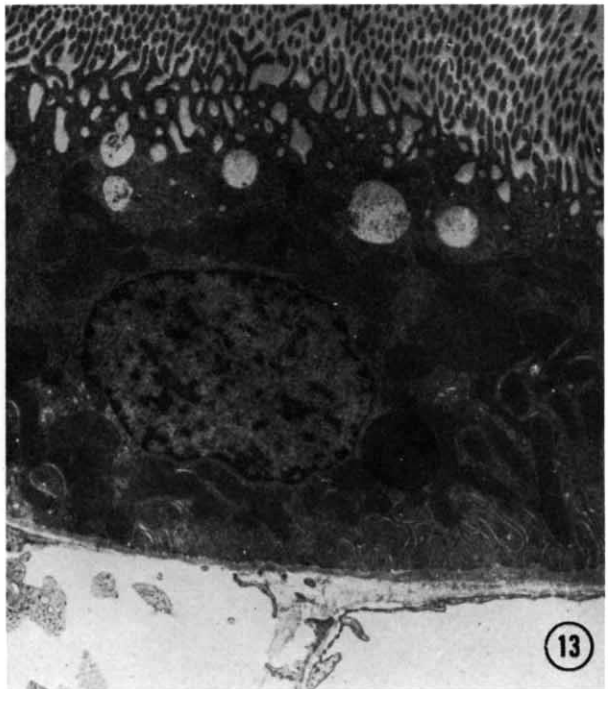

Fig. 10. *Electron micrograph of proximal tubule of rat receiving 9 mg/100 g sodium oxalate 1 hour prior to perfusion.* Note flocculent material located within the lumen, some of which is stained with pyroantimonate (×6580).

Fig. 11. *Electron micrograph of glomerulus from cortex of rat which was fixed 1 hour after receiving 5 mg/100 g sodium oxalate.* The tissue was treated with pyroantimonate. Stain product is located in urinary (Bowman's) space around podocytes (×7425).

Fig. 12. *Electron micrograph of proximal tubule of rat given 9 mg/100 g sodium oxalate, perfused 1 hour later, treated with EGTA and then pyroantimonate.* No stain appears in tissue (×31,700).

Fig. 13. *Electron micrograph of proximal tubule of normal perfused rat stained with pyroantimonate.* No staining occurred (×7450).

A number of groups have used potassium pyroantimonate for the cytochemical demonstration of calcium and sodium in tissues [25, 31–35]. Each study describes variations concerning tissue examined, pH used, and point at which pyroantimonate is introduced to the tissue. Lewis and Knight [36] give a detailed discussion of the pitfalls of this technique. Pyroantimonate will complex with sodium, potassium, magnesium, and calcium ions. If used in the initial aldehyde fixative, soluble calcium, sodium, and magnesium ions in the tissue will be precipitated as well as those insoluble compounds, such as calcium oxalate, which can react with pyroantimonate. To prevent this less specific reaction, we left our experimental tissues in aldehyde solutions for several hours to several weeks and then washed in three changes of distilled water prior to cytochemical staining. This apparently removed the soluble ions, so that the material that did stain was presumed to be calcium for the following reasons: *(1)* Animals which had not received injections of sodium oxalate prior to pyroantimonate staining exhibited no reaction product anywhere. *(2)* Animals treated with EGTA to remove calcium prior to pyroantimonate staining had little or no stain product anywhere except on the large, multicrystalline aggregations in tubular lumens (this treatment eliminates the possibility that staining in oxalate-treated animals could be due to sodium or potassium because EGTA does not chelate them). *(3)* When we examined with the x-ray microprobe crystals in tubular lumens that reacted with the pyroantimonate stain, we found calcium in large amounts, but no magnesium. The stain product associated with the crystals was identical in structure to that found in areas of the kidney with particulate material but devoid of polycrystalline aggregates. In addition, areas of tissue with no stain product scanned with the microprobe were found to be calcium-free.

The initial location of crystals formed within kidney tubules has been a matter of some discussion. Jordan, Finlayson, and Luxemberg [23] reported that rats injected with sodium oxalate formed calcium oxalate polycrystalline particles from 5 to 20 μ in diameter throughout the medulla and renal cortex in intratubular spaces. Vermeulen [11] and Malek and Boyce [37] found that the renal cortex was always less involved than was the medulla, which typically was more heavily studded with microcalculi nearer the papillary tip. This represents one of the most notable differences between our one-injection acute model and the more traditional chronic administration of lithogen models because the cortex is heavily involved in the early post-injection periods. Wright and Hodgkinson [38] found in rats that calcium oxalate crystals were attached to the basement membrane of tubule cells, though most crystals were located in tubule lumen. In the model described here, all crystals were present in the tubular lumen in early stages, whether in cortex or medulla, and none were located in the interstitium.

Cornelius and Moulton [17] proposed that calculous mucoid material may have originated as a secretory product of renal tubular cells. Resnick and Boyce believe that matrix substance A is probably of renal origin. It is detectable immunologically in renal tissue with calculi as well as it is in renal tissue containing only crystals [19]. They suggest that an early step in the formation of stones may be the binding of calcium by proteinaceous materials. In our studies, cellular membranous material is invariably found within the tubules of oxalate-treated animals, and it always formed a part of the crystal. This membranous material may be a source of some of the substances found in urine and associated with stones. Some of it may come from senescent cells of the tubular epithelium, and some may come from the sloughing of cell surface components of tubular cells because pieces of aberrant microvillus-like material are consistently found near crystalline material. Some may also be derived from intracellular membranes (Fig. 8). Similar findings have been described in mice fed a chronic lithogenic diet [22].

Our results demonstrate that earliest formation of calcium oxalate crystals within the intratubular lumen is a complex event. In contrast to calcium oxalate crystal formation in vitro, the formation of such crystals in the kidney involves, at the least, an undefined interaction between calcium, oxalate, cellular membranes, and other components. Construction of a crystal in this experimental model involves massive mobilization of calcium, presumably related to oxalate excretion. These complex with cellular membranes derived from tubular cells to form an organized crystalline array. Whether individual cells are killed in this process is not clear. Equally unclear is the origin of the cellular membranes involved in the organization of the crystal. Our data suggest that calcium is complexed with the microvillous membranes, possibly with the anionic portions of the cell coat, but the role played by the luminal vacuolar system and other cytoplasmic membranes is less certain.

Our hypothesis is that early formation of crystals is a phenomenon which involves only cellular lumi-

nal membranes. Although formation of such crystals may cause cellular damage or death, such events are secondary and not necessarily related to crystal formation. Further work is underway to test this concept.

Acknowledgments

This research was funded by NIH Research Grant #AM 20586-01. Drs. R. Bulger, B. Finlayson, S. Coleman, and P. Johnson gave technical guidance and suggestions. The Veteran's Administration Hospital in Gainesville, Florida, provided the electron microscope facility, and the Departments of Material Sciences and Microbiology and Cell Science at the University of Florida provided us with the use of their facilities. Ms. J. Duggan and Mr. E. J. Jenkins gave technical assistance during certain phases of this study.

Reprint requests to Dr. R. L. Hackett, Department of Pathology, School of Medicine, University of Florida, Gainesville, Florida 32610, USA.

References

1. LONSDALE K: Human stones. *Science* 159:1199–1207, 1968
2. PRIEN EL, PRIEN EL JR: Composition and structure of urinary stone. *Am J Med* 45:654–672, 1968
3. COE FL: *Nephrolithiasis, Pathogenesis and Treatment*. Chicago, Year Book Medical Publishers, Inc., 1978, chapter 2
4. HODGKINSON A: *Oxalic Acid in Biology and Medicine*. London, Academic Press, 1977
5. HAGLER L, HERMAN RH: Oxalate metabolism II. *Am J Clin Nutr* 26:882–889, 1973
6. RICHARDSON KE: Endogenous oxalate synthesis in male and female rats. *Toxicol Appl Pharmacol* 7:507–515, 1965
7. DOREMUS RH: Crystal growth and agglomeration in solution, in *Urolithiasis: Physical Aspects*, edited by FINLAYSON B, HENCH LC, SMITH LH, Washington, D.C., National Academy of Science, 1972, pp. 193–202
8. FINLAYSON B: Calcium stones: Some physical and clinical aspects, in *Calcium Metabolism in Renal Failure and Nephrolithiasis*, edited by DAVID DS, New York, John Wiley and Sons, Inc., 1977, pp. 337–382
9. HENCH LL: Factors in protein-mineral epitaxis, in *Urolithiasis: Physical Aspects*, edited by FINALYSON B, HENCH LL, SMITH LH, Washington, D.C., National Academy of Science, 1972, pp. 203–213
10. PAK CYC: Physiochemical and clinical aspects of nephrolithiasis, in *Colloquium on Renal Lithiasis*, edited by FINLAYSON B, THOMAS WC JR, Gainesville, Florida, University Presses of Florida, 1976, pp. 257–275
11. VERMEULEN CW: Calculogenesis and stone triggering, in *Urolithiasis: Physical Aspects*, edited by FINLAYSON B, HENCH LL, SMITH LH, Washington, D.C., National Academy of Science, 1972, pp. 237–242
12. DOREMUS RH, TEICH S, SILVIS PX: Crystallization of calcium oxalate from synthetic urine. *Invest Urol* 15:469–472, 1978
13. PRIEN EL JR: Calcium oxalate renal stones. *Ann Rev Med* 26:173–179, 1975
14. GARDNER GL, DOREMUS RH: Crystal growth inhibitors in human urine: Effect on calcium oxalate kinetics. *Invest Urol* 15:478–485, 1978
15. FINLAYSON B, REID F: The expectation of free and fixed particles in urinary stone disease. *Invest Urol* 15:442–448, 1978
16. BOYCE WH, GARVEY FK: The amount and nature of the organic matrix in urinary calculi: A review. *J Urol* 76:213–227, 1956
17. CORNELIUS CE, MOULTON JE: Ruminant urolithiasis: II. Histochemical studies in experimental ovine calculosis. *J Urol* 89:223–227, 1960
18. BOYCE WH: Organic matrix of human urinary concretions. *Am J Med* 45:673–683, 1968
19. RESNICK MI, BOYCE WH: Spherical calcium bodies in stone-forming urine. *Invest Urol* 15:449–451, 1978
20. EL-SAYED K, COSSLETT VE: Investigation of the microstructure of kidney stones (oxalate type) by high voltage electron microscopy and electron diffraction. *Experientia* 33:919–921, 1977
21. MALEK RS, BOYCE WH: Observations on the ultrastructure and genesis of urinary calculi. *J Urol* 117:336–341, 1977
22. KAWADA T, NODA S, ETO K: Scanning electron microscopic study on the developmental process of renal oxalate stone. *Jpn J Urol* 67:822–838, 1976
23. JORDAN WR, FINLAYSON B, LUXEMBERG M: Kinetics of early time calcium oxalate nephrolithiasis. *Invest Urol* 15:465–472, 1978
24. VAN'T RIET B, BOWE, RL: Formation and maintenance of reproducible calcium oxalate deposits in rat kidneys, in *Colloquium on Renal Lithiasis*, edited by FINLAYSON B, THOMAS WC JR, Gainesville, Florida, University Presses of Florida, 1976, pp. 168–172
25. OBERC MA, ENGEL WK: Ultrastructural localization of calcium in normal and abnormal skeletal muscle. *Lab Invest* 36:566–577, 1977
26. WATANABE T: Histochemical studies on mucosubstances in urinary stones. *Tohoku J Exp Med* 107:345–357, 1972
27. GRIFFITH LD, BULGER RE, TRUMP BF: Ultrastructure of the functioning kidney. *Lab Invest* 16:220–246, 1967
28. MCDOWELL EM, TRUMP BF: Histologic fixatives suitable for diagnostic light and electron microscopy. *Arch Pathol Lab Med* 100:405–414, 1976
29. SPURR AR: A low-viscosity epoxy resin embedding medium for electron microscopy. *J Ultrastruct Res* 26:31–43, 1969
30. REYNOLDS ES: The use of lead citrate at high pH as an electron opaque stain in electron microscopy. *J Cell Biol* 17:208–212, 1963
31. BULGER RE: Use of potassium pyroantimonate in the localization of sodium ions in rat kidney tissue. *J Cell Biol* 40:79–94, 1969
32. DEBBAS G, HOFFMAN L, LANDON EJ, HUSWITZ L: Electron microscopic localization of calcium in vascular smooth muscle. *Anat Rev* 182:447–472, 1975
33. LEGATO MJ, LANGER GA: The subcellular localization of calcium ion in myocardium. *J Cell Biol* 41:401–423, 1969
34. REITH EJ, BOYDE A: Histochemical and electron probe analysis of secretory ameloblasts of developing rat molar

teeth. *Histochemistry* 55:17–26, 1978
35. SPICER SS, HARDIN JH, GREENE WB: Nuclear precipitates in pyroantimonate-osmium tetroxide-fixed tissues. *J Cell Biol* 39:216–221, 1968
36. LEWIS PR, KNIGHT DP: *Staining Methods for Sectioned Material*. North-Holland, Amsterdam, 1977
37. MALEK RS, BOYCE WH: Intranephronic calculosis: Its significance and relationship to matrix in nephrolithiasis. *J Urol* 109:551–555, 1973
38. WRIGHT RJ, HODGKINSON A: Oxalic acid, calcium, and phosphorus in the renal papilla of normal and stone forming rats. *Invest Urol* 9:369–375, 1972